Impaired muscle force production and higher fatigability in a mouse model of sickle cell disease

Benjamin Chatel, Christophe Hourdé, Julien Gondin, Alexandre Fouré, Yann Le Fur, Christophe Vilmen, Monique Bernard, Laurent Messonnier, David Bendahan

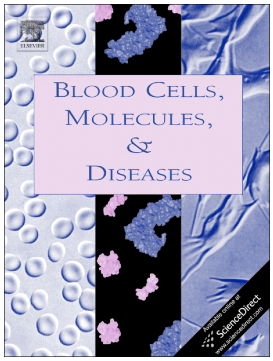

Impaired muscle force production and higher fatigability in a mouse model of sickle cell disease

Benjamin Chatel, Christophe Hourdé, Julien Gondin, Alexandre Fouré, Yann Le Fur, Christophe Vilmen, Monique Bernard, Laurent A. Messonnier, David Bendahan

PII: S1079-9796(16)30207-8
DOI: doi: 10.1016/j.bcmd.2017.01.004
Reference: YBCMD 2143

To appear in: *Blood Cells, Molecules and Diseases*

Received date: 28 September 2016
Accepted date: 9 January 2017

Please cite this article as: Benjamin Chatel, Christophe Hourdé, Julien Gondin, Alexandre Fouré, Yann Le Fur, Christophe Vilmen, Monique Bernard, Laurent A. Messonnier, David Bendahan , Impaired muscle force production and higher fatigability in a mouse model of sickle cell disease. The address for the corresponding author was captured as affiliation for all authors. Please check if appropriate. Ybcmd(2017), doi: 10.1016/j.bcmd.2017.01.004

Impaired muscle force production and higher fatigability in a mouse model of sickle cell disease

Benjamin Chatel[a], Christophe Hourdé[b], Julien Gondin[a,1], Alexandre Fouré[a], Yann Le Fur[a], Christophe Vilmen[a], Monique Bernard[a], Laurent A. Messonnier[a,b], David Bendahan[a]

[a]Aix-Marseille Univ, CNRS, CRMBM, Marseille, France

[b]Université Savoie Mont Blanc, Laboratoire Interuniversitaire de Biologie de la Motricité, EA7424, F-73000 Chambéry, France

[1]Present address: Institut NeuroMyoGène, Université Claude Bernard Lyon, UMR CNRS 5310 – INSERM U1217, 69100 VILLEURBANNE

Correspondence

Benjamin CHATEL

Centre de Résonance Magnétique Biologique et Médicale

Faculté de Médecine, 27 Boulevard Jean Moulin

13385 Marseille Cedex 05

benjamin.chatel@live.fr

Running title

Muscle function in sickle cell mice

Abbreviations

FTI: force-time integral
HbAA: control form
HbAS: heterozygous form of sickle cell disease
HbS: sickle hemoglobin
HbSS: homozygous form of sickle cell disease
MHC: myosin heavy chain
MRI: magnetic resonance imaging
Pf: peak force
RBC: red blood cell
$RFD_{initial}$: initial rate of force development
RFD_{max}: maximal rate of force development
SCD: sickle cell disease
$t_{1/2\ relax}$: half-time of force relaxation

Abstract

Skeletal muscle function has been scarcely investigated in sickle cell disease (SCD) so that the corresponding impact of sickle hemoglobin is still a matter of debate. The purpose of this study was to investigate muscle force production and fatigability in SCD and to identify whether exercise intensity could have a modulatory effect. Ten homozygous sickle cell (HbSS), ten control (HbAA) and ten heterozygous (HbAS) mice were submitted to two stimulation protocols (moderate and intense) to assess force production and fatigability. We showed that specific maximal tetanic force was lower in HbSS mice as compared to other groups. At the onset of the stimulation period, peak force was reduced in HbSS and HbAS mice as compared to HbAA mice. Contrary to the moderate protocol, the intense stimulation protocol was associated with a larger decrease in peak force and rate of force development in HbSS mice as compared to HbAA and HbAS mice. These findings provide *in vivo* evidence of impaired muscle force production and resistance to fatigue in SCD. These changes are independent of muscle mass. Moreover, SCD is associated with muscle fatigability when exercise intensity is high.

Key words

Rate of force development, muscle mass, exercise intensity, muscle volume.

Introduction

Sickle cell disease (SCD) is an inherited hemoglobin disorder characterized by the production of an abnormal hemoglobin S (HbS). The main pathological signs of the disease are a chronic hemolytic anemia and painful vaso-occlusive crises [1]. Skeletal muscle function has been reported to be impaired as a result of the pathophysiological manifestations of SCD. Indeed, maximal strength of forearm and respiratory muscles as well as peak power of locomotory muscles have been shown to be impaired in SCD patients [2; 3; 4; 5]. The reduced muscle strength reported in SCD mouse models (Berk and/or Townes) [6; 7; 8; 9; 10; 11] further supports the muscle dysfunction in SCD. While several potential accounting factors have been evoked with respect to the muscle dysfunction in SCD, they are still debated. The attractive hypothesis of a reduced muscle mass [2] has been put forth given that myocytes atrophy has recently been observed in SCD patients [12]. However, on the basis of body composition measurements, Dougherty *et al.* [3] suggested that the impaired muscle strength could not totally be explained by a reduced muscle volume. Along the same line, the reduced grip test performance reported in SCD mice was not linked to a reduced lean body mass [8]. These two latter studies suggest that the dampened muscle force production capacity in SCD cannot be exclusively related to muscle atrophy. A second hypothesis is related to central factors [2]. This is based on the fact that SCD patients displayed a 42% lower surface electromyography activity, suggesting an impaired muscle fibers recruitment [2]. However, this difference was not statistically significant. Deep tissue hyperalgesia has been proposed as an additional hypothesis given that analgesia improved muscle strength in SCD mice [6; 7; 9]. However, although analgesia did improve muscle function, the analgesic-treated SCD mice still displayed a reduced muscle strength as compared to their control counterparts [9]. Considering the multiple manifestations of SCD, one could hypothesize that skeletal muscle alterations could modulate muscle contraction and account for, at least to some extent, the well-acknowledged lower muscle force production. However, this hypothesis has never been tested so far.

Based on patients' reports [13; 14] and on performances during physical activities [15], fatigue has recently been suggested as a major symptom in SCD [13; 14], but this aspect remains controversial. In addition to hematological and cardiorespiratory limitations, it was suggested that alterations in skeletal muscle function could take part to the overall fatigue reported by SCD patients [16]. From a muscular point of view, fatigue has been defined as a reduction in the force generating capacity of the neuromuscular system, regardless of the level of force required [17]. Recently, Waltz et al. [2] reported a normal exercise-induced muscle fatigability in SCD patients as compared to control subjects. In their study, the reduction in maximal voluntary contraction (defined as fatigability) was reported for a 50%-maximal voluntary contraction exercise intensity [2] which could be considered as too moderate to distinguish patients and controls given the relationship between fatigability and exercise intensity [18]. In order to properly address this issue, it would be of interest to assess muscle fatigability in SCD for various exercise intensities. Considering that acute intense exercise could be harmful for SCD patients [19], we chose to investigate these parameters in a mouse model of the disease [20].

In the present study, we aimed at determining muscle force production and fatigability in response to different exercise intensities in a mouse model of SCD. In order to address the issue of potential confounding factors such as muscle atrophy, central factors and physical activity level, we used electrically induced contractions and quantified muscle mass and volume in strickly sedentary mice. In this study, we aimed at determining whether the

presence of HbS would be associated with impaired i) muscle force production and ii) resistance to fatigue and whether these effects would be dependent to exercise intensity.

Materials and Methods

Animal care and feeding

Investigations were performed in the Townes model of humanized SCD mice [B6;129-Hba$^{tm1(HBA)Tow}$Hbb$^{tm2(HBG1,HBB_n)\ Tow}$/Hbb$^{tm3(HBG1,HBB)Tow}$/J] (Jackson Laboratory, Stock number 013071) [6; 20; 21]. These mice do not express mouse hemoglobin but a human mutated hemoglobin. One mutation has been designed with the human hemoglobin α-gene and the second with i) the human ^{A}γ-globin gene and ii) sickle hemoglobin (β^{S}) or human wild-type beta globin (β^{A}) for SCD and control mice, respectively. Mice were identified through PCR genotyping of mouse-tail DNA according to the Jackson Laboratory's recommendations. SCD mice recapitulate several hematologic phenotypes of human SCD (anemia, reticulocytosis, leukocytosis, sickling) and have liver as well as kidney disorders [6; 20; 21].

Five-month-old (males) HbAA (control, n = 10), HbAS (heterozygous form of SCD, n = 10) and HbSS (homozygous form of SCD, n = 10) mice were used in this study conducted in agreement with the French guidelines for animal care and in conformity with the European convention for the protection of vertebrate animals used for experimental purposes and institutional guidelines n° 86/609/ CEE November 24, 1986. All animal experiments were approved by the Institutional Animal Care Committee of Aix-Marseille University (permit number: 01835.02). Mice were housed in an environment-controlled facility (12–12 h light–dark cycle, 22 °C) and received water and standard food *ad libitum*.

Animal preparation

Mice were initially anesthetized in an induction chamber (Equipement vétérinaire, Minerve, France) using 4% isoflurane in 33% O_2 and 66% N_2O. After the whole left lower hindlimb was shaved, electrode cream for electromyography was applied at the knee and heel regions to optimize electrical stimulation. Anesthetized animal was placed supine within a home-built cradle designed especially for the strictly noninvasive investigation of posterior hindlimb muscles function [22; 23]. The setup integrates an ergometer consisting of a foot pedal coupled to a force transducer and two rod-shaped transcutaneous surface electrodes (one located above the knee and the other under the heel) connected to an electrical stimulator (Digitimer, Ltd., Model DS7A, Welwyn Springs, UK). The foot was positioned on the ergometer pedal that was adjusted to have a 90° flexion ankle joint. Corneas were protected from drying by applying ophthalmic cream, and the animal's head was placed in a home-built facemask supplied continuously with isoflurane throughout the experiment for anesthesia maintenance. Animal body temperature was controlled and maintained at physiological temperature during anesthesia using a feedback loop, including an electrical heating blanket (Prang & Partner, Pfungen, Switzerland), a temperature control unit (ref. no. 507137; Harvard Apparatus), and a home-built rectal thermometer constructed with a NTC thermistor SMC series (ref no. NCP18XW220J03RB-2.2K; Murata, Kyoto, Japan). Breath rate was controlled throughout the protocol and isoflurane concentration was adjusted to keep the breath rate between 100 and 130 breath·min^{-1} (1.25 – 1.75 % isoflurane).

Study design

The non-invasivness of our setup permit to test mice twice over a one-week period in order to assess muscle mechanical performance using two different stimulation protocols

(moderate and intense) performed in a random order. Muscle volume and T_2 values were quantified at rest using magnetic resonance imaging (MRI).

MRI data acquisition and processing

Investigations were performed using a 47/30 Biospec Avance MR system (Bruker, Karlsruhe, Germany) equipped with a Bruker 120-mm BGA12SL (200 mT/m) gradient insert. Ten consecutive non-contiguous axial scout slices (1 mm thickness, spaced 1 mm) covering the region from the knee to the ankle were selected across the lower hindlimb.
RARE images of these slices (Rare factor = 4, effective echo time = 22.52 ms, actual echo time = 19.597 ms, repetition time = 1000 ms, 6 accumulations, 42 x 42 mm field of view, 256 x 192 matrix size, acquisition time = 4 min 48 s) were recorded at rest in order to assess muscle volume. The posterior hindlimb muscles region was manually delineated on each slice and then muscle volume (mm^3) was calculated as the sum of the four volumes included between the five consecutive largest slices. The reproductibility of this method has already been demonstrated [22].

Multiecho T_2-weighted images of these slices (16 echo times equally spaced from 11.79 ms to 188.67 ms; 2020-ms repetition time; one accumulation; 30 x 30 mm field of view; 256 x 128 matrix size; total acquisition time = 4.3 min) were recorded at rest. T_2-weighted images were processed in order to generate T_2-maps on a pixel-by-pixel basis by fitting the ^{1}H-MRI data with a single exponential function. Because of imperfect refocusing (hermite refocusing pulse), even echoes were excluded from the analysis. Mean T_2 values for the posterior hindlimb muscles were measured on T_2 maps and averaged for the three consecutive largest slices by manually outlining regions of interest.

Maximal tetanic force measurement

Transcutaneous stimulation intensity was first elicited with square-wave pulses (0.5 ms duration). The individual maximal stimulation intensity was determined by progressively increasing the stimulus intensity until there was no further increase in force. This intensity was then maintained to assess maximal tetanic force using tetanic stimulation (duration = 0.5 s, frequency = 150 Hz). Maximal tetanic force was determined on the basis of the maximal force amplitude and was evaluated twice over a one-week period (before each stimulation protocol). The highest value recorded was considered as the maximal tetanic force and was also expressed with respect to posterior hindlimb muscles weight to obtain specific maximal tetanic force.

Stimulation protocols and force measurement

The transcutaneous stimulation protocol consisted in 6 min of repeated isometric contractions electrically induced with square wave pulses (0.5 ms duration) at the individual maximal stimulation intensity. One stimulation protocol was set at 0.5 Hz (moderate protocol) and the other at 2 Hz (intense protocol).

Force data acquisition and processing

Analog electrical signal coming out from the force transducer was amplified with a home-built amplifier (gain = 70 dB, 0–5 kHz bandwidth, Operational amplifier AD620; Analog Devices, Norwood, MA), converted to a digital signal, monitored and recorded on a personal computer using the Powerlab 35/series system (AD Instruments, Oxford, United Kingdom). Peak force (Pf, $mN.g^{-1}$) and force-time integral (FTI, $mN.s.g^{-1}$) were calculated for each

contraction (Fig 1) using the LabChart software (AD Instruments, Oxford, United Kingdom) and expressed with respect to posterior hindlimb muscles weight. Initial rate of force development ($RFD_{initial}$), maximal rate of force development (RFD_{max}) and half-time of force relaxation ($t_{1/2\ relax}$) were determined for each contraction using a MATLAB (MathWorks, USA) routine as described in Fig 1. $RFD_{initial}$ and RFD_{max} refer to the force signal slopes measured during the first 20 ms of contraction and within ± 10 ms the half-time of force contraction, respectively. $t_{1/2\ relax}$ refers the time delay between the peak force and the half-relaxation. The first contraction of both protocols was used to evaluate initial Pf, FTI, $RFD_{initial}$, RFD_{max} and $t_{1/2\ relax}$.

Each parameter was averaged every 4 s, except for FTI for which data were summed over 4 s to assess force production. For each protocol, a fatigue index was quantified. Because of the differences of Pf time-course between moderate and intense protocols, the fatigue index was differently calculated in each protocol. During the moderate protocol, the fatigue index was calculated as the difference between the mean Pf recorded during the first and the last 4 seconds of contraction and expressed as a percentage of the value recorded during the first 4 seconds. For the intense protocol, the fatigue index corresponded to the difference between the maximal and the last values of Pf, expressed as a percentage of the maximal value. In the same way, $RFD_{initial}$, RFD_{max} and $t_{1/2\ relax}$ changes were also calculated during both protocols as the difference between the mean of the corresponding parameter recorded during the first and the last 4 seconds of contraction and expressed as a percentage of the value recorded during the first 4 seconds. During the intense protocol, a staircase index was also quantified considering Pf. It corresponds to the difference between the minimal value recorded during the first two minutes of stimulation and the maximal value and was expressed as a percentage of the minimal value recorded during the first thirty seconds.

Tissue withdrawal

Mice were anesthetized intra-peritoneally with a Ketamine (110 mL/kg) – Xylazine (10 mL/kg) mixture. Soleus, plantaris, gastrocnemius, tibialis anterior and extensor digitorum longus muscles were carefully dissected before mice were submitted to a cervical dislocation. Each muscle was then weighted (wet weight). The posterior hindlimb muscles weight, corresponding to the sum of soleus, plantaris and gastrocnemius muscles weights was used for the normalization of force parameters. Tibialis anterior and extensor digitorum longus muscles weights were also summed to determine the anterior hindlimb muscles weight.

Myosin heavy chain (MHC) isoforms distribution

After the whole gastrocnemius of 6 HbAA, 6 HbAS and 6 HbSS mice were crushed with mortar and pestle immersed in liquid nitrogen, approximately 30 mg of muscle was homogenized in 500 µL of buffer (NaH_2PO_4 200 mM, Na_2HPO_4 200 mM, Magnesium acetate 4 mM, Aprotinine 10 µg/mL, EGTA 1mM) with a tissue homogenizer (Polytron PT 1600 E, Kinematica, Switzerland). After 0.1 % triton was added, samples were incubated 45 minutes at 4°C and then centrifuged (1 h, 10 000 g, 4°C). The pellet was resuspended (NaCl 0.3 M, NaH_2PO_4 0.1 M, Na_2HPO_4 0.05 M, $Na_4P_2O_7$ 0.01 M, $MgCl_2$ 1mM, EDTA 10 mM, ß-mercaptoethanol 1.4 mM, pH 6.5). After a one-hour incubation (4°C), samples were centriguged (15 min, 10 000 g, 4°C). The supernatant were diluted 1:1 (v/v) with glycerol and stored at -20°C [24].

MHCs were separated on 4% polyacrylamide stacking gel and 8% polyacrylamide

running gel both containing 30% glycerol [25] using the Bio-Rad mini-protean Tetra cell system as previously described [24]. The gels were migrated for 36 h at 70 V and the temperature was maintained at 4°C. The gels were silver stained [26] and different isoforms previously identified [24] were monitored using the ChemiDoc™ XRS+ System (Bio-Rad Laboratories). Signal intensity was quantified using the Image Lab™ Software (Bio-Rad Laboratories) and expressed as a percentage of total MHC signal.

For MHC distribution analysis, only the gastrocnemius was analyzed since i) gastrocnemius muscle represent more than 80 % of total posterior hindlimb muscles weight and, ii) it has been previously demonstrated that this stimulation protocol involved principally the gastrocnemius muscle [22].

Statistical analysis

Data are presented as means ± standard deviation. Statistical analyses were performed with Statistica software version 9 (StatSoft, Tulsa, OK, USA). Normality was checked using a Kolmogorov–Smirnov test. One-way ANOVA was used to compare anatomic parameters, T_2 values, MHC isoforms distribution and the changes in force parameters observed during the protocol. Repeated measures ANOVA were used to identify potential group differences in force parameters at the onset of the stimulation protocol (the first contraction of both protocols corresponded to the repeated measure). Repeated measures ANOVA were also used to compare time-courses of force parameters. When a main effect or a significant interaction (indicating that the time-effect on the dependent variable is different among groups) was found, a Newman–Keuls post-hoc analysis was performed. Significance was accepted when $p < 0.05$.

Results

Anatomical properties and T_2 values

Anatomical data are summarized in table 1. Body weight, posterior and anterior hindlimb muscle weights and posterior hindlimb muscles volume measured by MRI (illustrated in Fig 2 and showed in table 1) were not statistically different among groups ($p > 0.05$). In addition, T_2 values of posterior hindlimb muscles were not different between HbAA (26.1 ± 1.1 ms), HbAS (27.1 ± 1.6 ms) and HbSS (27.2 ± 2.0 ms) mice ($p > 0.05$).

Muscle force parameters at the onset of the stimulation protocol

Absolute maximal tetanic force (Fig 3A) was significantly reduced in HbSS as compared to HbAA mice (–13%, $p < 0.05$). The 8%-decrease in comparison with the HbAS group did not reach the level of significance ($p > 0.05$). The specific maximal tetanic force (per g of muscle mass) was significantly reduced in HbSS mice as compared to both HbAA (–21%, $p < 0.001$) and HbAS (–17 %, $p < 0.001$) groups (Fig 3B).

The force parameters evaluated for the first twitch of both protocols are summarized in Table 2. Pf was significantly reduced in both HbSS ($p < 0.001$, –36%) and HbAS ($p < 0.01$, –24%) as compared to HbAA mice (421 ± 119 $mN.g^{-1}$). FTI was also significantly lower in both groups ($p < 0.01$) than in control mice. Both $RFD_{initial}$ and RFD_{max} were reduced in both HbSS and HbAS groups ($p < 0.05$) while the $t_{1/2\ relax}$ was longer in HbSS and HbAS mice as compared to control mice ($p < 0.05$, +10%).

Time-courses of muscle force parameters during moderate and intense stimulation protocols

As illustrated in Figs 4A and 4C, time-courses of Pf and FTI were fairly stable throughout the moderate protocol, although we observed a significant time-effect for both parameters ($p < 0.001$) which could be due to the slight decrease at the onset of the stimulation protocol. On the contrary, the intense protocol led to a totally different pattern with a significant time effect too (Figs 4B and 4D, $p < 0.001$). The time-courses of Pf and FTI were biphasic with an initial increase and a peak reached after a 90-s contraction period. Then both variables progressively decreased until the end of the stimulation period. Overall, we observed that both HbSS and HbAS mice developed a lower Pf as compared to HbAA mice during both the moderate ($p < 0.01$ and $p < 0.05$, respectively) and the intense ($p < 0.001$ and $p < 0.01$, respectively) stimulation protocols. The FTI time-course differed regarding the groups and the stimulation protocol. During the moderate protocol, only the HbSS mice displayed lower values as compared to the HbAA mice (Fig 4C, $p < 0.05$). On the contrary, both HbSS ($p < 0.001$) and HbAS ($p < 0.01$) mice had a reduced FTI during the intense protocol (Fig 4D). Interestingly, the HbAS mice had both a higher Pf and FTI as compared to the HbSS mice during the intense protocol only ($p < 0.05$). During the moderate stimulation protocol, we did observe no significant time x group interaction ($p > 0.05$) either for the fatigue index or the FTI change among the different groups (table 3, $p > 0.05$). On the contrary, for the intense protocol, we found a significant time x group interaction ($p < 0.001$) with fatigue index and FTI change being significantly larger in HbSS mice as compared to both HbAS ($p < 0.05$ and $p < 0.01$, respectively) and HbAA ($p < 0.01$, table 3) mice. In addition, the staircase index was significantly lower in the HbSS mice as compared to the HbAS group ($p < 0.01$) and tended to be lower in HbSS as compared to HbAA mice ($p = 0.063$, table 3).

During the moderate protocol, HbAS and HbSS mice presented slower initial ($RFD_{initial}$, $p < 0.01$, Fig 5A) and maximal (RFD_{max}, $p < 0.05$, Fig 5C) rates of force development as compared to the HbAA group. Similarly, during the intense protocol (Figs 5B and 5D), HbSS mice displayed slower $RFD_{initial}$ ($p < 0.05$) and RFD_{max} ($p < 0.01$) as compared to HbAA mice. The comparative analysis between the HbAS and the HbAA mice only disclosed a slower RFD_{max} in the HbAS group ($p < 0.05$) whereas the $RFD_{initial}$ was not significantly different. Althought we observed a group x time interaction for $RFD_{initial}$ and RFD_{max} during the moderate protocol (Figs 5A and 5C), both $RFD_{initial}$ and RFD_{max} changes were not statistically different among groups (table 3). On the contrary, during intense protocol, both $RFD_{initial}$ and RFD_{max} changes were significantly larger in HbSS mice in comparison to other groups (table 3, $p < 0.01$ and $p < 0.001$, respectively).

Regarding the post-stimualtion relaxation phase, the half-time of force relaxation ($t_{1/2\ relax}$, Figs 6A and 6B) was not affected by group, whatever the stimulation protocol (table 2).

MHC isoforms distribution

Three different MHC isoforms were separated from the whole gastrocnemius homogenates in the three groups (Fig 7B) given that our methods did not distinguish type IIa and IIx MHC isoforms. As illustrated in Fig 7A, no difference was observed regarding the MHC isoforms distribution among groups.

Discussion

In the present study, we aimed at characterizing muscle function in a humanized SCD mouse model and at identifying whether exercise intensity could modulate the potentially impaired force production and fatigability. We mainly found that force production capacity was impaired in SCD mice and so independently of muscle mass. We also identified that HbSS mice displayed a higher fatigability throughout the intense exercise, whereas exercise-induced muscle fatigue was unchanged during the moderate stimulation protocol. Interestingly, the muscle function profile in HbAS mice was almost systematically intermediate between the HbSS and the HbAA groups.

Muscle force production

One of our key findings is related to the impaired muscle force production capacity in SCD mice which is supported by several converging results. The absolute and specific maximal tetanic forces were reduced in the SCD mice similarly to the Pf and FTI measured at the onset of the stimulation protocol (table 2) and throughout moderate and intense exercises (Fig 4). The lower maximal force production (–21% for specific maximal tetanic force) reported here in SCD mice is in accordance with previous studies conducted in humans [3; 4] and in mouse models [6; 7; 9]. As compared to our results, all the animal model studies reported a similar reduction in grip test performance [6; 7; 9; 10; 11] (–18 and –28% for overall and forelimb strength, respectively [6]) while studies conducted in humans indicated a reduced maximal voluntary contraction of forearm muscles (–27% [2], –16% [3] and –23% [4]). In addition, regardless of exercise intensity, the presence of HbS was associated with a significantly slower RFD indicating an impaired kinetics of force development in SCD mice.

Considering the well acknowledged relationship between force production and muscle size [27], Waltz et al. [2] proposed that the force alterations in SCD would be accounted for the muscle atrophy. In our study, muscle mass and volume investigations clearly ruled this hypothesis out. The present results are in agreement with Dougherty et al. [3] who previously suggested that the force production deficit found in SCD patients could not totally be explained by anthropometric alterations. Alternatively, possible modulations of force production capacity by central factors involved in muscle activation were suggested by Waltz et al. [2] since SCD patients displayed a 42% lower (but not statistically significant) surface electromyography activity. However, central factors cannot be considered as accounting factors in our study given that force was electrically induced (with maximal intensities) in anesthetized mice. Taken together, our results emphasize alteration of muscle function associated with HbS, and so independently of muscle atrophy and central factors involved in muscle activation. In other words, the muscle dysfunction we have quantified in SCD mice could be, at least partly, attributed to altered muscle properties.

In that respect, some of our results would argue in favor of a particular muscle fiber type distribution in SCD mice. Indeed, it has been shown that both staircase phenomenon [28] and RFD [29; 30] were clearly higher in type II as compared to type I fibers. The reduced staircase index (even if the difference was not significant with HbAA mice) and RFD we observed in SCD mice would then suggest a shift toward a lower proportion of type II fibers in those animals in agreement with the reduced proportion of type II fibers reported in SCD patients [12]. However, no difference in MHC isoforms distribution was found in the present study (for the gastrocnemius muscle), suggesting a regular contractile phenotype in SCD mice. Considering that i) we observed no alteration in MHC isoforms distribution in

SCD mice, and that ii) fiber type distribution has been poorly correlated with maximal force production [27], we can assume that other accounting factors should explain the impaired muscle force production capacity we observed in SCD mice.

The pro-inflammatory status, which has been previously described in SCD [31; 32] could also be evoked. It has been shown that an inflammatory status can directly affect contractile function (reducing maximal force and RFD) thereby resulting in muscle weakness [33]. In order to assess a potential inflammatory status, we measured T_2-relaxation times at rest using MRI. In both humans and animal models, it has been shown that T_2 values could change in a variety of pathophysiological conditions including among others, edema, necrosis, fatty infiltration and inflammation [34; 35]. The unchanged T_2-relaxation in the SCD mice could rule out muscle damage and inflammation as accounting factors of the impaired muscle force production capacity in SCD mice. Accordingly, neither inflammation nor necrosis has been reported in muscle tissue of SCD patients [12].

Considering that force relaxation and staircase phenomenon were reported to depend on sarcoplasmic reticulum function [18] and the Ca^{2+}/calmodulin-dependent pathway [28], respectively, the longer $t_{1/2\ relax}$ and lower staircase index we measured in SCD mice could illustrate a potential Ca^{2+} handling deficiency. These potentially impaired calcium-mediated mechanisms have to be analyzed in the light of a recent study showing than the total deletion of calpain-1 (a calcium activated protease) in HbSS mice (Townes) was related to an increased grip force [11]. Although our hypothesis is speculative, it has to be kept in mind that, oxidative stress, which has been well-described in SCD [36; 37], is also known to reduce myofibrillar Ca^{2+} sensitivity and to impair Ca^{2+} uptake by the sarcoplasmic reticulum, leading to the deterioration of muscle function [38]. Further studies should be performed in order to address this issue.

The heterozygous form of SCD (HbAS or sickle cell trait) is characterized by a smaller proportion of HbS [39]. Interestingly, muscle force parameters of HbAS mice were almost systematically intermediate between the HbSS and HbAA mice. This observation would suggest that muscle dysfunction is proportional to HbS content and further supports the idea of a deleterious effect of HbS on muscle tissue and function, as already observed in humans [12].

Muscle fatigability

In the present study, we illustrated that the fatigability variables (changes in Pf, FTI and RFD) recorded during the moderate protocol were not abnormal for the SCD mice (table 3). These results are consistent with those of Waltz *et al*. [2] who found a similar force reduction in SCD patients submitted to a light fatigue protocol as compared to healthy controls. Interestingly, the similar force reduction measured by Waltz et al. [2] (–17% for SCD patients) and in our moderate protocol (–21% for SCD mice) could indicate that these exercises were comparable in terms of intensity. Taking together, these studies suggest that a moderate exercise is not particularly stressful for the muscle function in SCD. Along the same line, previous studies indicated that moderate exercises did not induce clinical, hemorheological and inflammatory complications in SCD patients [40; 41].

On the contrary to what we observed during the moderate exercise, the intense stimulation protocol induced a larger fatigability in SCD as compared to controls. The corresponding variables i.e. the changes in Pf, FTI and RFD were significantly higher in HbSS mice as compared to both the HbAS and HbAA counterparts. Considering that this type of exercise has a large metabolic impact in terms of phosphocreatine and glycogen beakdown [42; 43] and given that the corresponding by-products i.e., inorganic phosphate

and protons [42; 43] have been incriminated in disruption of muscle function (i.e. force production and RFD) [18; 44; 45; 46], a metabolic defect might be considered as a potential accounting factor of the higher fatigability in SCD. Supportive of this hypothesis, SCD is associated with anemia (a well-known accounting factor of fatigue [47]) [1], arterial desaturation [48; 49] and impaired muscle oxidative potential [12], which collectively contribute to limit muscle oxygen supply and utilization and potentially exacerbate non-oxidative ATP production thereby leading to marked intracellular acidosis and inorganic phosphate accumulation [50]. Further studies should be performed in order to address this issue.

Conclusion

In summary, in the present study, we provided functional evidences of a significantly impaired muscle function in SCD mice which is independent of muscle mass and central factors. Interestingly, the corresponding abnormalities regarding muscle weakness and fatigability are exacerbated by an intense exercise. Given that muscle strength, RFD and fatigue were described as predictors of functional capacity in elderly people and patients with various diseases [14; 51; 52; 53], these factors could explain the poor quality of life in SCD patients. Further investigations would be required to describe the underlying muscle structural alterations and/or metabolic mechanisms involved in muscle weakness and fatigability in SCD.

Acknowledgments

This study was supported by Centre National de la Recherche Scientifique (CNRS UMR 7339) and a grant of Société Française de Myologie and Genzyme. This work was performed by a laboratory member of France Life Imaging network (grant ANR-11-INBS-0006). The funders had no role in study design, data collection and analysis, decision to publish, or preparation of the manuscript.

References

[1] D.C. Rees, T.N. Williams, M.T. Gladwin, Sickle-cell disease. Lancet 376 (2010) 2018-31.

[2] X. Waltz, A. Pichon, N. Lemonne, et al., Normal muscle oxygen consumption and fatigability in sickle cell patients despite reduced microvascular oxygenation and hemorheological abnormalities. PLoS One 7 (2012) e52471.

[3] K.A. Dougherty, J.I. Schall, A.J. Rovner, V.A. Stallings, B.S. Zemel, Attenuated maximal muscle strength and peak power in children with sickle cell disease. Journal of pediatric hematology/oncology 33 (2011) 93-7.

[4] H. Moheeb, Y.A. Wali, M.S. El-Sayed, Physical fitness indices and anthropometrics profiles in schoolchildren with sickle cell trait/disease. Am J Hematol 82 (2007) 91-7.

[5] D.G. Ohara, G. Ruas, I.A. Walsh, S.S. Castro, M. Jamami, Lung function and six-minute walk test performance in individuals with sickle cell disease. Braz J Phys Ther 18 (2014) 79-87.

[6] G. Calhoun, L. Wang, L.E. Almeida, et al., Dexmedetomidine ameliorates nocifensive behavior in humanized sickle cell mice. Eur J Pharmacol 754 (2015) 125-33.

[7] D.R. Kohli, Y. Li, S.G. Khasabov, et al., Pain-related behaviors and neurochemical alterations in mice expressing sickle hemoglobin: modulation by cannabinoids. Blood 116 (2010) 456-65.

[8] P.L. Capers, H.I. Hyacinth, S. Cue, et al., Body composition and grip strength are improved in transgenic sickle mice fed a high-protein diet. J Nutr Sci 4 (2015) e6.

[9] D. Vang, J.A. Paul, J. Nguyen, et al., Small-molecule nociceptin receptor agonist ameliorates mast cell activation and pain in sickle mice. Haematologica 100 (2015) 1517-25.
[10] J. Lei, B. Benson, H. Tran, S.F. Ofori-Acquah, K. Gupta, Comparative Analysis of Pain Behaviours in Humanized Mouse Models of Sickle Cell Anemia. PLoS ONE 11 (2016) e0160608.
[11] J.O. Nwankwo, J. Lei, J. Xu, et al., Genetic inactivation of calpain-1 attenuates pain sensitivity in a humanized mouse model of sickle cell disease. Haematologica 101 (2016) e397-e400.
[12] M. Ravelojaona, L. Feasson, S. Oyono-Enguelle, et al., Evidence for a profound remodeling of skeletal muscle and its microvasculature in sickle cell anemia. Am J Pathol 185 (2015) 1448-56.
[13] S. Ameringer, W.R. Smith, Emerging biobehavioral factors of fatigue in sickle cell disease. J Nurs Scholarsh 43 (2011) 22-9.
[14] S. Ameringer, R.K. Elswick, Jr., W. Smith, Fatigue in Adolescents and Young Adults With Sickle Cell Disease: Biological and Behavioral Correlates and Health-Related Quality of Life. Journal of pediatric oncology nursing : official journal of the Association of Pediatric Oncology Nurses (2013).
[15] R.M. Millis, F.W. Baker, L. Ertugrul, R.M. Douglas, L. Sexcius, Physical performance decrements in children with sickle cell anemia. Journal of the National Medical Association 86 (1994) 113-6.
[16] L.A. Callahan, K.F. Woods, G.A. Mensah, et al., Cardiopulmonary responses to exercise in women with sickle cell anemia. American journal of respiratory and critical care medicine 165 (2002) 1309-16.
[17] B. Bigland-Ritchie, J.J. Woods, Changes in muscle contractile properties and neural control during human muscular fatigue. Muscle Nerve 7 (1984) 691-9.
[18] R.H. Fitts, Cellular mechanisms of muscle fatigue. Physiol Rev 74 (1994) 49-94.
[19] C. Martin, V. Pialoux, C. Faes, et al., Does physical activity increase or decrease the risk of sickle cell disease complications? Br J Sports Med (2015).
[20] L.C. Wu, C.W. Sun, T.M. Ryan, et al., Correction of sickle cell disease by homologous recombination in embryonic stem cells. Blood 108 (2006) 1183-8.
[21] J. Hanna, M. Wernig, S. Markoulaki, et al., Treatment of sickle cell anemia mouse model with iPS cells generated from autologous skin. Science 318 (2007) 1920-3.
[22] B. Giannesini, C. Vilmen, Y. Le Fur, et al., A strictly noninvasive MR setup dedicated to longitudinal studies of mechanical performance, bioenergetics, anatomy, and muscle recruitment in contracting mouse skeletal muscle. Magn Reson Med 64 (2010) 262-70.
[23] C. Gineste, J.M. De Winter, C. Kohl, et al., In vivo and in vitro investigations of heterozygous nebulin knock-out mice disclose a mild skeletal muscle phenotype. Neuromuscul Disord 23 (2013) 357-69.
[24] O. Agbulut, Z. Li, V. Mouly, G.S. Butler-Browne, Analysis of skeletal and cardiac muscle from desmin knock-out and normal mice by high resolution separation of myosin heavy-chain isoforms. Biol Cell 88 (1996) 131-5.
[25] R.J. Talmadge, R.R. Roy, Electrophoretic separation of rat skeletal muscle myosin heavy-chain isoforms. J Appl Physiol (1985) 75 (1993) 2337-40.
[26] H. Blum, H. Beier, H.J. Gross, Improved silver staining of plant proteins, RNA and DNA in polyacrylamide gels. ELECTROPHORESIS 8 (1987) 93-99.

[27] S.W. Trappe, T.A. Trappe, G.A. Lee, D.L. Costill, Calf muscle strength in humans. Int J Sports Med 22 (2001) 186-91.
[28] G. Zhi, J.W. Ryder, J. Huang, et al., Myosin light chain kinase and myosin phosphorylation effect frequency-dependent potentiation of skeletal muscle contraction. Proc Natl Acad Sci U S A 102 (2005) 17519-24.
[29] J. Farup, H. Sorensen, T. Kjolhede, Similar changes in muscle fiber phenotype with differentiated consequences for rate of force development: endurance versus resistance training. Hum Mov Sci 34 (2014) 109-19.
[30] P. Aagaard, E.B. Simonsen, J.L. Andersen, P. Magnusson, P. Dyhre-Poulsen, Increased rate of force development and neural drive of human skeletal muscle following resistance training. J Appl Physiol (1985) 93 (2002) 1318-26.
[31] S.A. Akohoue, S. Shankar, G.L. Milne, et al., Energy expenditure, inflammation, and oxidative stress in steady-state adolescents with sickle cell anemia. Pediatr Res 61 (2007) 233-8.
[32] J.D. Belcher, C.J. Bryant, J. Nguyen, et al., Transgenic sickle mice have vascular inflammation. Blood 101 (2003) 3953-9.
[33] G.J. Pinniger, T. Lavin, A.J. Bakker, Skeletal muscle weakness caused by carrageenan-induced inflammation. Muscle Nerve 46 (2012) 413-20.
[34] T. Marqueste, B. Giannesini, Y.L. Fur, P.J. Cozzone, D. Bendahan, Comparative MRI analysis of T2 changes associated with single and repeated bouts of downhill running leading to eccentric-induced muscle damage. J Appl Physiol (1985) 105 (2008) 299-307.
[35] G. Zaccagnini, A. Palmisano, T. Canu, et al., Magnetic Resonance Imaging Allows the Evaluation of Tissue Damage and Regeneration in a Mouse Model of Critical Limb Ischemia. PLoS One 10 (2015) e0142111.
[36] E. Nur, B.J. Biemond, H.M. Otten, D.P. Brandjes, J.J. Schnog, Oxidative stress in sickle cell disease; pathophysiology and potential implications for disease management. Am J Hematol 86 (2011) 484-9.
[37] E.N. Chirico, V. Pialoux, Role of oxidative stress in the pathogenesis of sickle cell disease. IUBMB Life 64 (2011) 72-80.
[38] F.H. Andrade, M.B. Reid, D.G. Allen, H. Westerblad, Effect of hydrogen peroxide and dithiothreitol on contractile function of single skeletal muscle fibres from the mouse. J Physiol 509 (Pt 2) (1998) 565-75.
[39] R.N. Wrightstone, T.H. Huisman, A. van der Sar, Qualitative and quantitative studies of sickle cell hemoglobin in homozygotes and heterozygotes. Clin Chim Acta 22 (1968) 593-601.
[40] E. Balayssac-Siransy, P. Connes, N. Tuo, et al., Mild haemorheological changes induced by a moderate endurance exercise in patients with sickle cell anaemia. British journal of haematology 154 (2011) 398-407.
[41] P. Barbeau, K.F. Woods, L.T. Ramsey, et al., Exercise in sickle cell anemia: effect on inflammatory and vasoactive mediators. Endothelium : journal of endothelial cell research 8 (2001) 147-55.
[42] L.J. Haseler, R.S. Richardson, J.S. Videen, M.C. Hogan, Phosphocreatine hydrolysis during submaximal exercise: the effect of FIO2. J Appl Physiol (1985) 85 (1998) 1457-63.
[43] R.F. Fregosi, J.A. Dempsey, Effects of exercise in normoxia and acute hypoxia on respiratory muscle metabolites. J Appl Physiol (1985) 60 (1986) 1274-83.

[44] C.R. Nelson, R.H. Fitts, Effects of low cell pH and elevated inorganic phosphate on the pCa-force relationship in single muscle fibers at near-physiological temperatures. Am J Physiol Cell Physiol 306 (2014) C670-8.
[45] E.P. Debold, Recent insights into the molecular basis of muscular fatigue. Med Sci Sports Exerc 44 (2012) 1440-52.
[46] R.H. Fitts, The cross-bridge cycle and skeletal muscle fatigue. J Appl Physiol (1985) 104 (2008) 551-8.
[47] W.J. Evans, C.P. Lambert, Physiological basis of fatigue. Am J Phys Med Rehabil 86 (2007) S29-46.
[48] C.T. Quinn, J.W. Sargent, Daytime steady-state haemoglobin desaturation is a risk factor for overt stroke in children with sickle cell anaemia. Br J Haematol 140 (2008) 336-9.
[49] B.N. Setty, M.J. Stuart, C. Dampier, D. Brodecki, J.L. Allen, Hypoxaemia in sickle cell disease: biomarker modulation and relevance to pathophysiology. Lancet 362 (2003) 1450-5.
[50] L.J. Haseler, C.A. Kindig, R.S. Richardson, M.C. Hogan, The role of oxygen in determining phosphocreatine onset kinetics in exercising humans. The Journal of Physiology 558 (2004) 985-992.
[51] J. Holviala, A. Hakkinen, M. Alen, et al., Effects of prolonged and maintenance strength training on force production, walking, and balance in aging women and men. Scand J Med Sci Sports 24 (2014) 224-33.
[52] C. Suetta, P. Aagaard, A. Rosted, et al., Training-induced changes in muscle CSA, muscle strength, EMG, and rate of force development in elderly subjects after long-term unilateral disuse. J Appl Physiol (1985) 97 (2004) 1954-61.
[53] T. Kjolhede, K. Vissing, D. Langeskov-Christensen, et al., Relationship between muscle strength parameters and functional capacity in persons with mild to moderate degree multiple sclerosis. Mult Scler Relat Disord 4 (2015) 151-8.

Figure legends

Fig 1. Time-course of force production during a typical single twitch.
Pf is the peak force and FTI (grey hatching) the force-time integral. $RFD_{initial}$ refers to the rate of force development measured during the first 20 ms of contraction. RFD_{max} is the rate of force development measured between the 10-ms before and the 10-ms after the half-time of force contraction points. $t_{1/2\ relax}$: half-time of force relaxation.

Fig 2. Typical axial magnetic resonance images representing hindlimb of HbAA (A), HbAS (B) and HbSS (C) mice.
Regions of interest drawn in black dashes correspond to the posterior area of the hindlimb selected for muscle volume measurements.

Fig 3. Absolute (A) and specific (B) maximal tetanic force.

Values are presented as mean ± SD. * and ***: significantly different from HbAA ($p < 0.05$ and $p < 0.001$, respectively). †††: significantly different from HbAS ($p < 0.001$). 10 HbAA (19.0 ± 0.7 weeks old), 10 HbAS (18.7 ± 0.6 weeks old) and 10 HbSS (18.3 ± 0.5 weeks old) male mice were studied.

Fig 4. Time-courses of peak force and force-time integral during moderate (A and C, respectively) and intense (B and D, respectively) stimulation protocols in HbAA (white), HbAS (grey) and HbSS (black) mice.
Values are presented as mean ± SD. *, ** and ***: Significantly different from HbAA ($p < 0.05$, $p < 0.01$ and $p < 0.001$, respectively). †: Significantly different from HbAS ($p < 0.05$). 10 HbAA (19.0 ± 0.7 weeks old), 10 HbAS (18.7 ± 0.6 weeks old) and 10 HbSS (18.3 ± 0.5 weeks old) male mice were studied.

Fig 5. Time-courses of initial and maximal rates of force development during moderate (A and C, respectively) and intense (B and D, respectively) stimulation protocols in HbAA (white), HbAS (grey) and HbSS (black) mice.
Values are presented as mean ± SD. * and **: significantly different from HbAA ($p < 0.05$ and $p < 0.01$, respectively). 10 HbAA (19.0 ± 0.7 weeks old), 10 HbAS (18.7 ± 0.6 weeks old) and 10 HbSS (18.3 ± 0.5 weeks old) male mice were studied.

Fig 6. Time-course of $t_{1/2\ relax}$ during moderate (A) and intense (B) stimulation protocols in HbAA (white), HbAS (grey) and HbSS (black) mice.
Values are presented as mean ± SD. 10 HbAA (19.0 ± 0.7 weeks old), 10 HbAS (18.7 ± 0.6 weeks old) and 10 HbSS (18.3 ± 0.5 weeks old) male mice were studied.

Fig 7. MHC isoforms distribution in HbAA (white), HbAS (grey) and HbSS (black) mice (A) and typical electrophoretic separation of gastrocnemius muscle MHC isoforms (B).
Values are presented as mean ± SD. n = 6.

Table 1. Anatomical parameters

	HbAA	HbAS	HbSS
Body weight (g)	32.4 ± 3.2	31.9 ± 3.4	31.2 ± 2.6
Posterior hindlimb muscles weight (mg)	150 ± 14	150 ± 15	166 ± 20
Anterior hindlimb muscles weight (mg)	57 ± 8	56 ± 6	58 ± 6
Posterior hindlimb muscles volume (mm^3)	154 ± 10	154 ± 12	160 ± 20

Data are presented as mean ± SD. Posterior hindlimb muscles weight corresponds to the sum of soleus, plantaris and gastrocnemius muscles weights. Anterior hindlimb muscles weight corresponds to the sum of tibialis anterior and extensor digitorum longus muscles weights. 10 HbAA (19.0 ± 0.7 weeks old), 10 HbAS (18.7 ± 0.6 weeks old) and 10 HbSS (18.3 ± 0.5 weeks old) male mice were studied.

Table 2. Force parameters at the onset of the stimulation protocols (measured on the first twitch of both protocols).

	HbAA	HbAS	HbSS
Pf ($mN.g^{-1}$)	421 ± 119	318 ± 73**	268 ± 67***
FTI ($mN.s.g^{-1}$)	48 ± 17	35 ± 11**	32 ± 8**
$RFD_{initial}$ ($mN.s^{-1}$)	915 ± 289	641 ± 275*	706 ± 257*
RFD_{max} ($mN.s^{-1}$)	1621 ± 439	1263 ± 303*	1243 ± 300*
$t_{1/2\ relax}$ (ms)	40 ± 4	44 ± 3*	44 ± 4*

Data are presented as mean ± SD. Pf: peak force, FTI: force-time integral, $RFD_{initial}$: initial rate of force development, RFD_{max}: maximal rate of force development, $t_{1/2\ relax}$: half-time of force relaxation. *, ** and ***: significantly different from HbAA mice ($p < 0.05$, $p < 0.01$ and $p < 0.001$, respectively). 10 HbAA (19.0 ± 0.7 weeks old), 10 HbAS (18.7 ± 0.6 weeks old) and 10 HbSS (18.3 ± 0.5 weeks old) male mice were studied.

Table 3. Changes in force parameters during moderate and intense stimulation protocols

	HbAA	HbAS	HbSS
Moderate protocol			
Fatigue index (%)	-18 ± 17	-18 ± 18	-21 ± 15
FTI change (%)	-35 ± 18	-32 ± 19	-28 ± 13
$RFD_{initial}$ change (%)	36 ± 18	34 ± 32	12 ± 19
RFD_{max} change (%)	7 ± 13	4 ± 17	-4 ± 16
$t_{1/2\ relax}$ change (%)	-10 ± 7	-12 ± 7	-8 ± 11
Intense protocol			
Fatigue index (%)	-69 ± 6	-73 ± 5	-78 ± 5** †
Staircase index (%)	53 ± 17	65 ± 23	37 ± 14^{t} ††
FTI change (%)	-53 ± 13	-56 ± 8	-70 ± 8** ††
$RFD_{initial}$ change (%)	-23 ± 12	-20 ± 23	-47 ± 13** ††
RFD_{max} change (%)	-52 ± 8	-54 ± 10	-70 ± 8*** †††
$t_{1/2\ relax}$ change (%)	26 ± 13	22 ± 19	12 ± 20

Data are presented as mean ± SD. $RFD_{initial}$: initial rate of force development, RFD_{max}: maximal rate of force development, $t_{1/2\ relax}$: half-time of force relaxation. ** and ***: significantly different from HbAA mice ($p < 0.01$ and $p < 0.001$, respectively). ^{t}: tends to be different from HbAA mice ($0.05 < p < 0.1$). †, †† and †††: significantly different from HbAS mice ($p < 0.05$, $p < 0.01$ and $p < 0.001$, respectively). 10 HbAA (19.0 ± 0.7 weeks old), 10 HbAS (18.7 ± 0.6 weeks old) and 10 HbSS (18.3 ± 0.5 weeks old) male mice were studied.

Figure 1

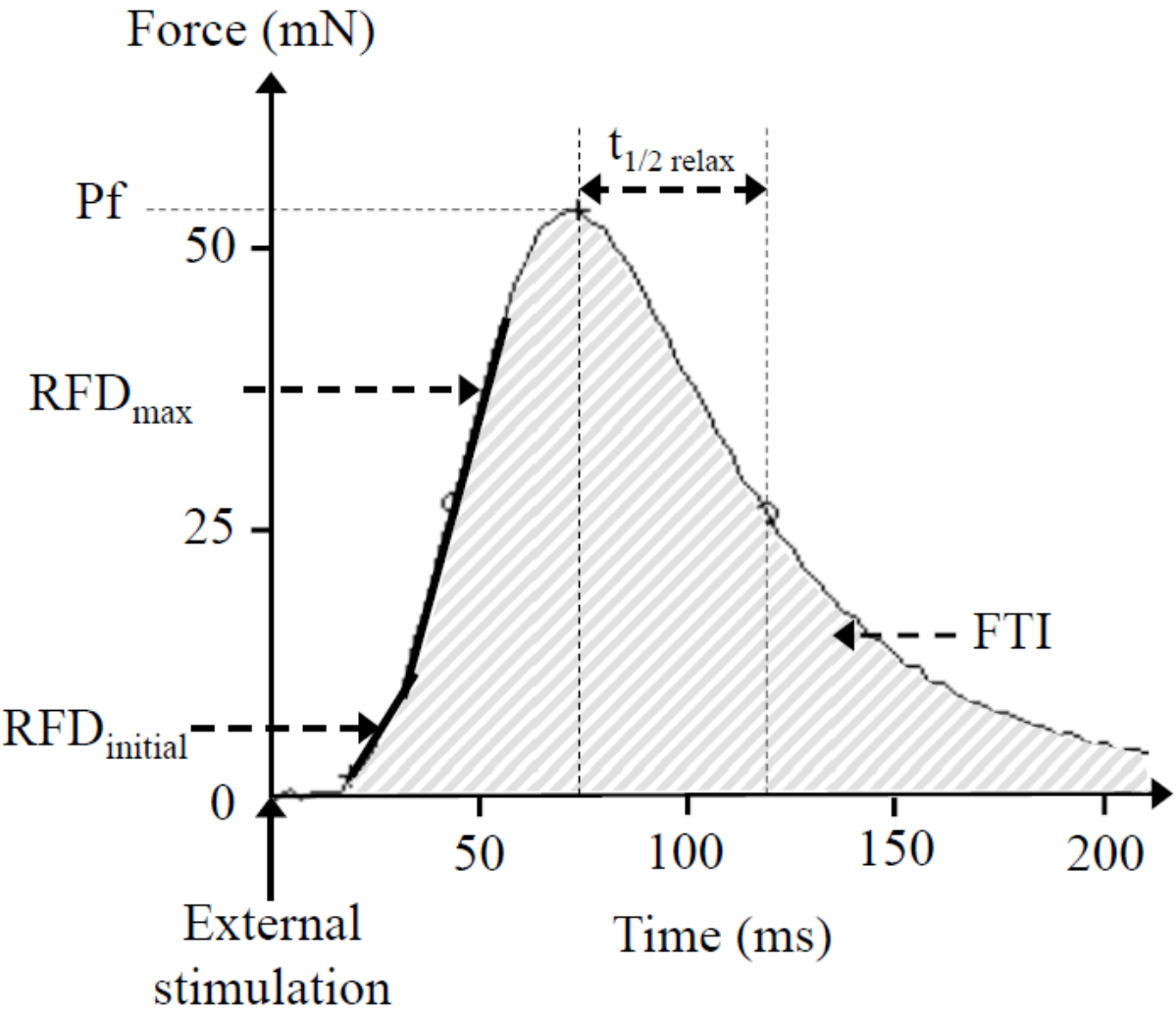

Figure 2

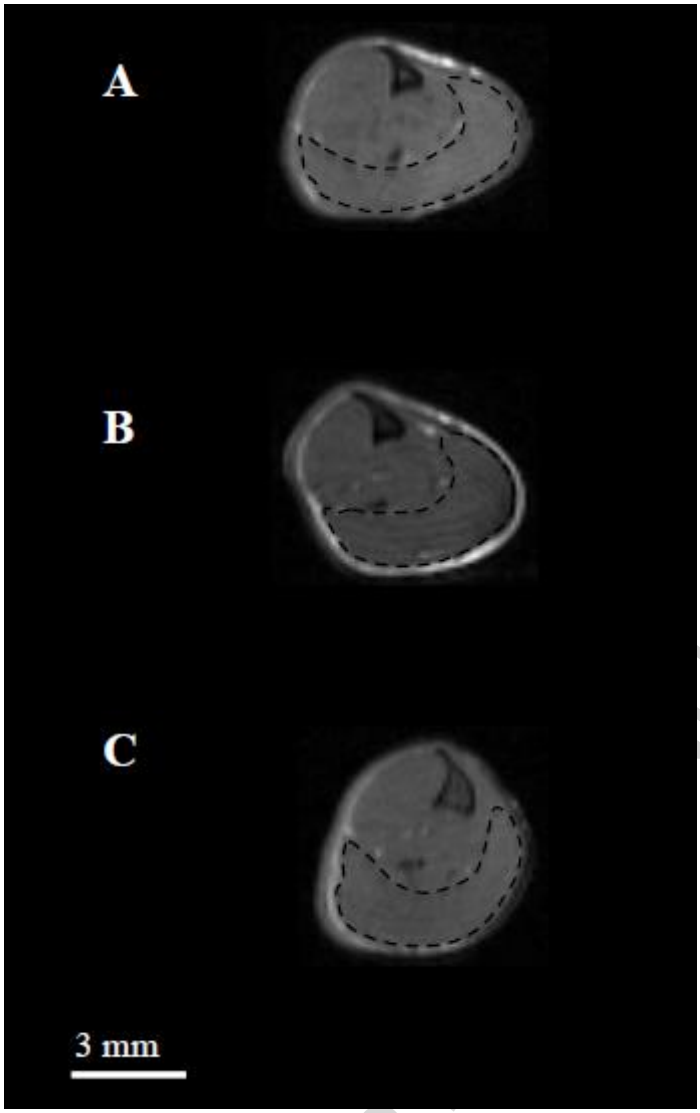

Figure 3

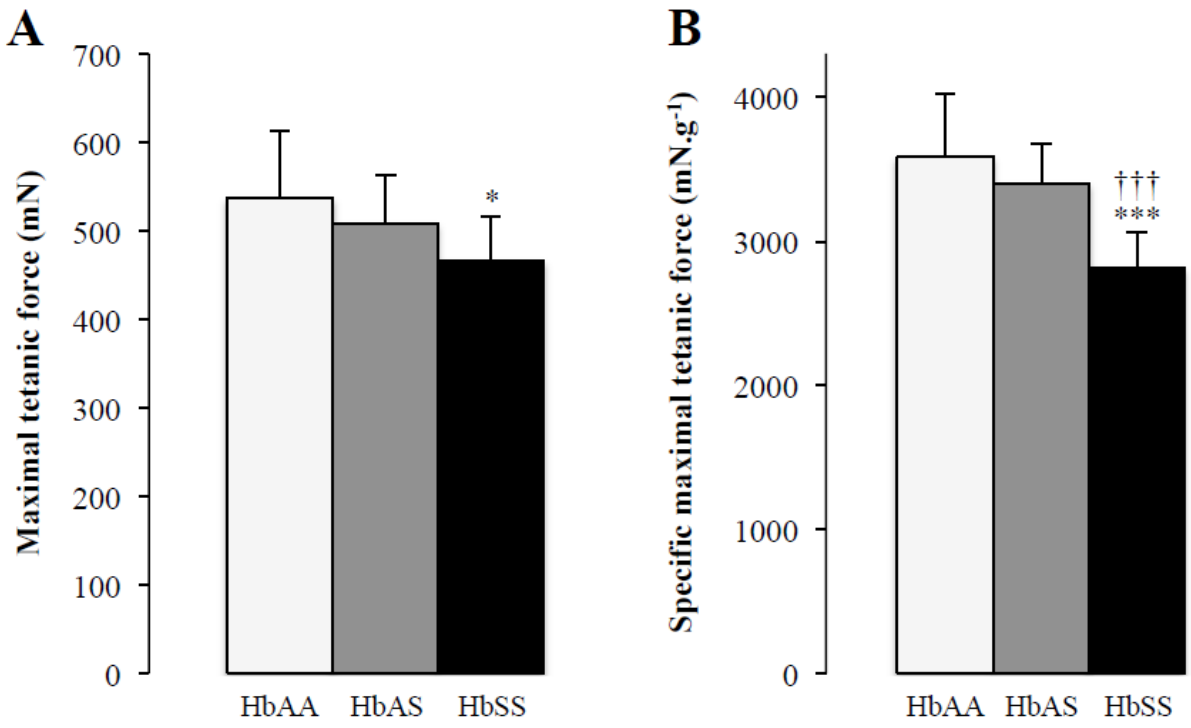

Figure 4

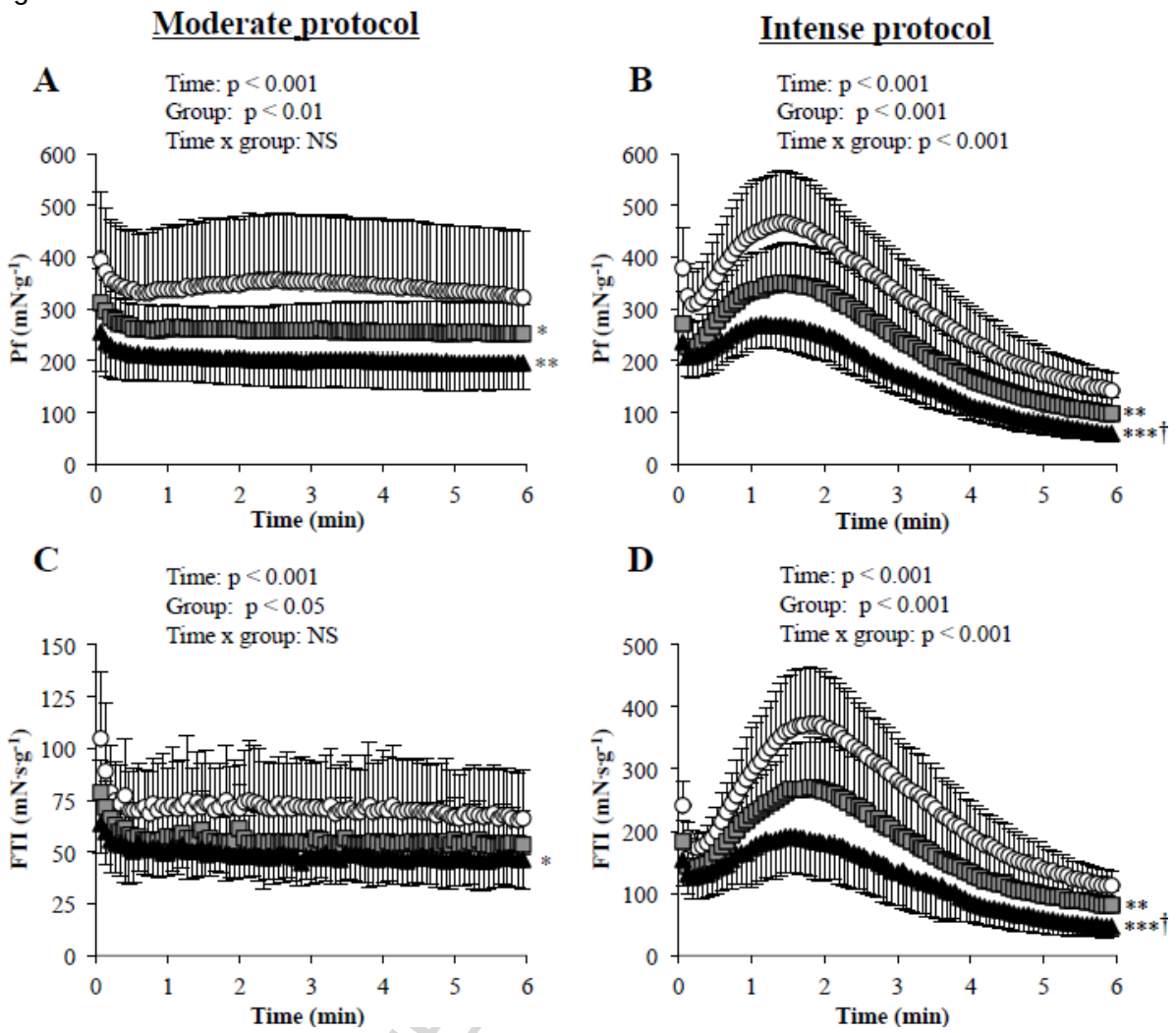

Figure 5

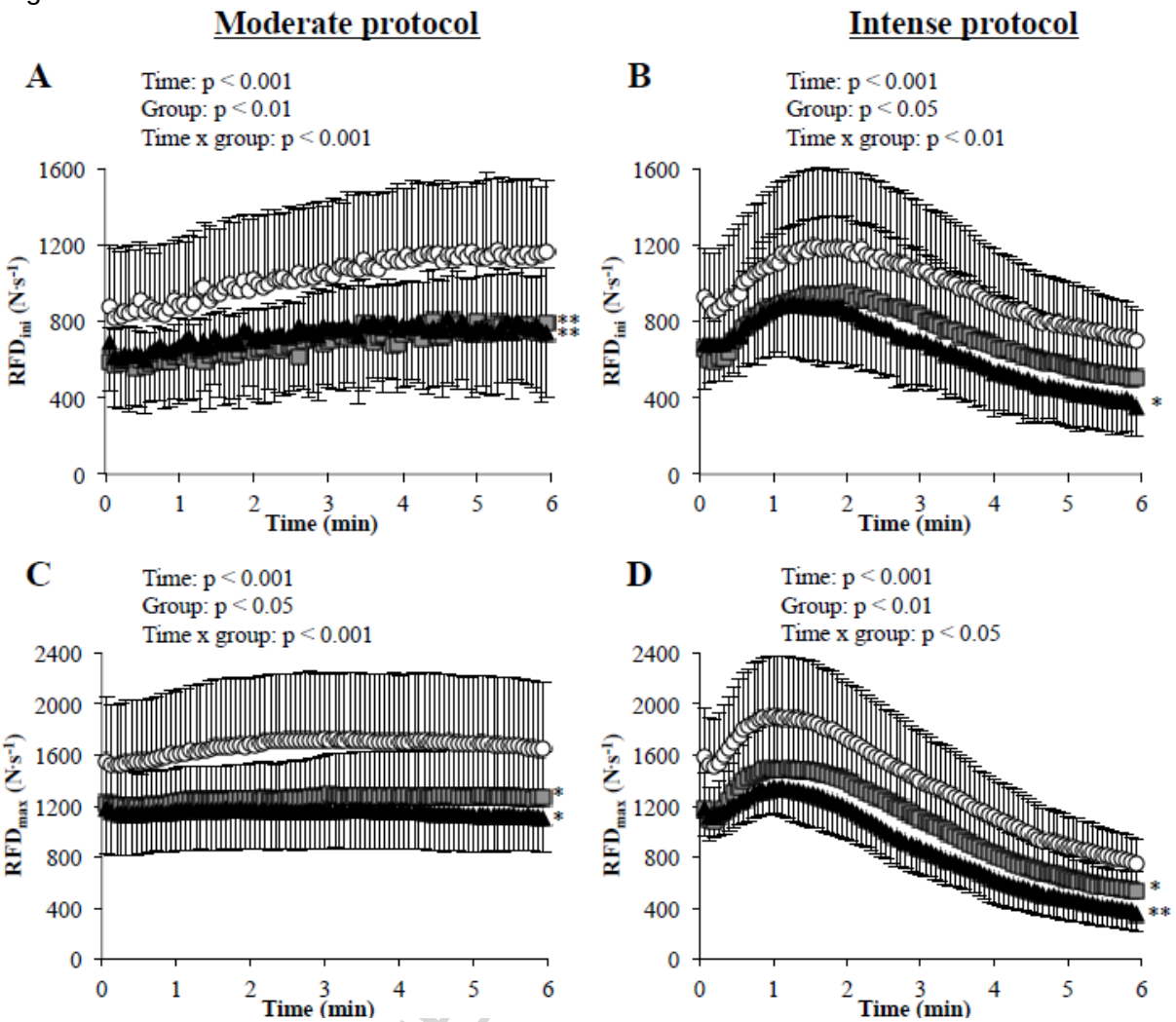

Figure 6

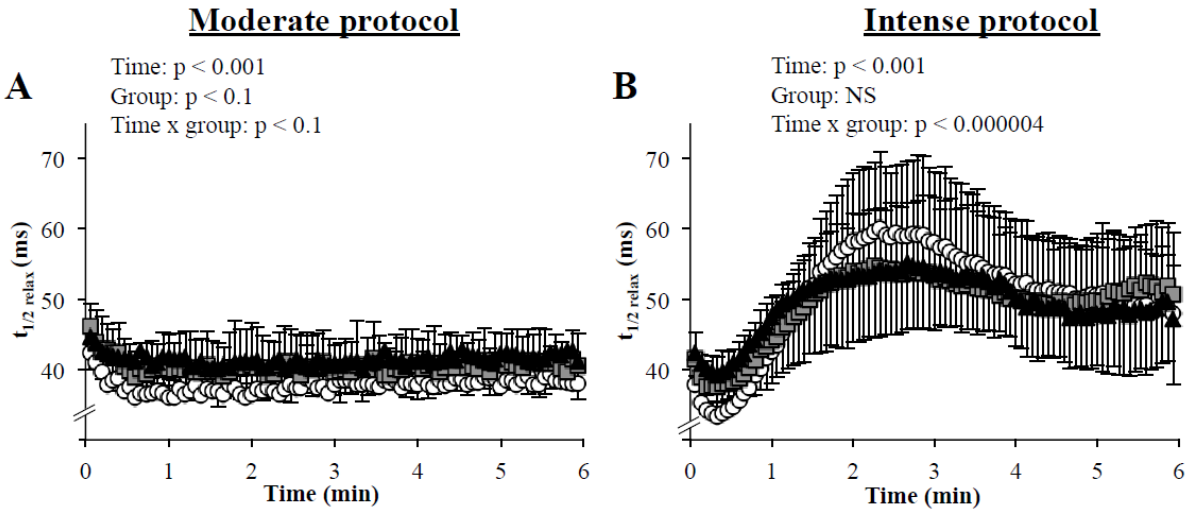

Figure 7